

## An improved capacity spectrum method for ATC-40

Yu-Yuan Lin and Kuo-Chun Chang<sup>\*,†</sup>

*Department of Civil Engineering, National Taiwan University, Taipei 106, Taiwan*

### SUMMARY

In order to account for the non-linear behavior of structures via non-linear static procedure, the capacity spectrum method has been adopted by ATC-40 for evaluation and retrofit of reinforced concrete buildings. For elastic-perfectly-plastic SDOF systems, the accuracy of the capacity spectrum method depends only on the acceleration response spectrum chosen to form the demand spectrum and the adopted model for calculating the equivalent viscous damping ratios. According to this method, the pseudo-acceleration response spectrum ( $PS_a$ ) is used to create the demand diagram. It is found that the ATC-40 procedure, using its Type A hysteretic model, may be inaccurate especially for systems with damping ratios greater than 10% and periods longer than 0.15 sec. In order to improve the accuracy of the capacity spectrum method, this study proposes to use the real absolute acceleration response spectrum ( $S_a$ ) instead of the  $PS_a$  to establish the demand diagram. The step-by-step procedure of the improved method and examples are implemented in this paper to illustrate the calculations of earthquake-induced deformations. In addition, three selected models of equivalent viscous damping are also compared in this paper to assess the accuracy of the model used in the ATC-40 procedure. Results show that the WJE damping model may be used by the capacity spectrum method to reasonably predict the inelastic displacements when the ductility demand ( $\mu$ ) of the structures is less than 4, whereas the damping model proposed by Kowalsky can be implemented when  $\mu > 4.0$ . Alternatively, the damping model proposed by Kowalsky may be used to calculate the equivalent viscous damping for the entire range of ductility. Copyright © 2003 John Wiley & Sons, Ltd.

KEY WORDS: capacity spectrum method; equivalent linear systems; absolute acceleration; pseudo-acceleration

### 1. INTRODUCTION

The capacity spectrum method (CSM), adopted in ATC-40 [1], was first introduced in the 1970s as a rapid evaluation procedure for assessing the seismic vulnerability of buildings [2–4]. This procedure compares the capacity of the structure in the form of a pushover curve

\* Correspondence to: Kuo-Chun Chang, Department of Civil Engineering, National Taiwan University, No. 1 Sec. 4, Roosevelt Road, Taipei 106, Taiwan.

† E-mail: ciekuo@ccms.ntu.edu.tw

Contract/grant sponsor: National Science Council, Taiwan; contract/grant number: NSC-90-2811-Z-002-003  
Contract/grant sponsor: Sinotech Engineering Consultant of Taiwan; contract/grant number: 6120

*Received 21 May 2002*

*Revised 30 September 2002 and 10 January 2003*

*Accepted 17 February 2003*

with demands on the structure in the form of an elastic response spectrum. The graphical intersection of the two curves approximates the response of the structure [2, 3, 5, 6]. In order to account for these effects of non-linear behavior of structures, equivalent viscous damping has been implemented to modify this elastic response spectrum to consider the inelastic behavior. Implied in the capacity spectrum method is that earthquake-induced deformation of a non-linear single-degree-of-freedom (SDOF) system can be approximately estimated by an iterative procedure of a sequence of equivalent linear SDOF systems. Therefore, it avoids the dynamic analysis of inelastic systems.

It should be noted that ATC-40 modified the capacity spectrum method by proposing its own method for determining the equivalent damping ratios. The ATC-40 method was based on an idealistic hysteretic model.

After the capacity spectrum method was proposed by ATC-40, Chopra and Goel [7, 8] pointed out that the procedure significantly underestimated the deformation for a wide range of periods when using the Type A idealized hysteretic damping model. An improved method using the inelastic response spectrum as the demand diagram was proposed by Fajfar [9] and Chopra and Goel [7, 8]. It should be noted that in actual practice, for existing reinforced concrete structures, the ATC-40 procedure uses the Type B and C damping values which result in substantially smaller damping ratios.

For elastic-perfectly-plastic SDOF systems, the accuracy of the capacity spectrum method depends only on: (a) the acceleration response spectrum chosen to form the demand spectrum; and (b) the adopted model of equivalent viscous damping. Although the errors generated above can be eliminated by using the inelastic response spectrum [7–9], the capacity spectrum method has the advantage of using the equivalent linear systems to predict the responses of non-linear systems.

According to the capacity spectrum method used in ATC-40, the pseudo-acceleration ( $PS_a$ ), an approximate acceleration response spectrum derived from the displacement response spectrum ( $S_d$ ), was used to create the demand diagram based on the relationship of  $PS_a = \omega^2 S_d$ , where  $\omega$  (Hz) represents the natural frequency of the systems. In this study it is found that such a situation will obviously lose the accuracy of iteration results, especially for systems with damping ratios greater than 10% and periods longer than 0.15 sec. To improve the accuracy of the capacity spectrum method without using the inelastic response spectrum, this paper suggests that the real acceleration response spectrum ( $S_a$ ) is used instead of the pseudo-acceleration response spectrum ( $PS_a$ ) to establish the demand diagram.

In addition, the equivalent viscous damping model plays another significant role in the capacity spectrum method. If the equivalent damping ratios of the equivalent linear systems cannot be determined appropriately, the displacement demand of structures will not be accurately obtained even when the real absolute acceleration response spectrum ( $S_a$ ) is used. For the purpose of determining the equivalent viscous damping ratios used in ATC-40 with reasonable accuracy, three equivalent viscous damping models are also discussed and compared in this paper.

## 2. EQUIVALENT LINEAR SYSTEMS

Figure 1 shows the force–deformation relationship of a bilinear SDOF system, where  $k$ ,  $\alpha$ ,  $f_y$ ,  $u_y$ ,  $u_{max}$  and  $\mu$  are the elastic stiffness, post-yield stiffness ratio, yield strength, yield displacement, and ultimate displacement, respectively.

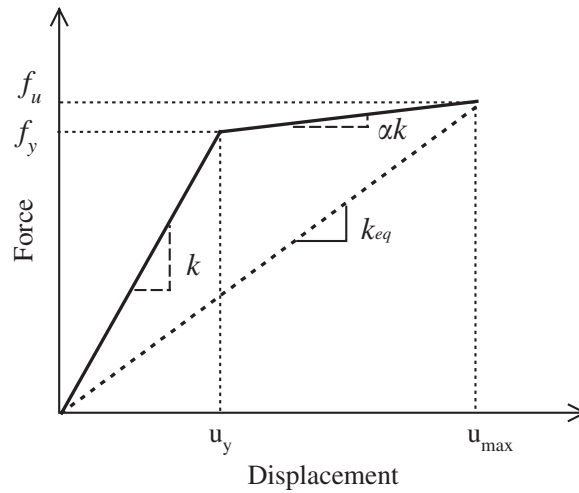


Figure 1. Force–displacement relationship of bilinear SDOF system.

ment, maximum displacement and ductility ratio ( $\mu = u_{\max}/u_y$ ), respectively. The maximum force and displacement response of the bilinear system can be estimated by an equivalent linear system [10–13] with secant stiffness  $k_{eq}$ , natural period  $T_{eq}$  and equivalent viscous damping ratio  $\zeta_{eq}$  [8], where

$$T_{eq} = T_n \sqrt{\frac{\mu}{1 + \alpha\mu - \alpha}} \quad (1)$$

$$\zeta_{eq} = \zeta_0 + \zeta_h; \text{ and } \zeta_h = \frac{1}{4\pi} \frac{E_D}{E_S} = \frac{2}{\pi} \frac{(\mu - 1)(1 - \alpha)}{\mu(1 + \alpha\mu - \alpha)} \quad (2)$$

In Equations (1) and (2),  $T_n$  = elastic natural vibration period of the bilinear system;  $\zeta_0$  = inherent damping ratio of the bilinear system vibrating within its linearly elastic range;  $\zeta_h$  = equivalent hysteretic damping ratio;  $E_D$  = energy dissipated in the bilinear system, i.e. enclosed area of the hysteretic loops; and  $E_S$  = strain energy of the system with stiffness  $k_{eq}$ . In ATC-40, a modified  $\zeta_{eq}$  is used as

$$\zeta_{eq} = \zeta_0 + \kappa \zeta_h \quad (3)$$

where  $\zeta_h$  is limited to 45%. The damping modification factor  $\kappa$  depends on the types of hysteretic behavior of the system [1]. Type A denotes hysteretic behavior with stable and full hysteresis loops. For such systems,  $\kappa = 1$  if  $\zeta_h \leq 16.25\%$ ,  $\kappa = 0.77$  if  $\zeta_h \geq 45\%$ , and  $\kappa$  = linear interpolation if  $16.25\% \leq \zeta_h \leq 45\%$ . Type C represents severely pinched loops; and the hysteretic behavior of the Type B system is between Type A and Type C. Furthermore, ATC-40 specifies three different procedures (Procedures A, B and C) to estimate the earthquake-induced deformation demand, all based on the same principles but different in their methods of implementation. Procedure A is suggested to be the best of the three procedures.

### 3. PSEUDO-ACCELERATION RESPONSE SPECTRUM ( $PS_a$ ) vs. ABSOLUTE ACCELERATION RESPONSE SPECTRUM ( $S_a$ )

In the capacity spectrum method of ATC-40, the ordinate of the pseudo-acceleration response spectrum ( $PS_a$ ) is used as the vertical axis and the ordinate of the displacement response spectrum ( $S_d$ ) is used as the horizontal axis to create the demand diagram. For a linear SDOF system with viscous damping and subjected to ground acceleration  $\ddot{u}_g(t)$ , the equation of motion is given as

$$m\ddot{u}(t) + c\dot{u}(t) + ku(t) = -m\ddot{u}_g(t) \quad (4)$$

where  $m$ ,  $c$ ,  $k$ ,  $\omega$  and  $\zeta$  are the mass, damping coefficient, stiffness, natural frequency and viscous damping ratio of the system, respectively;  $u(t)$ ,  $\dot{u}(t)$ ,  $\ddot{u}(t)$  and  $\ddot{u}'(t) = \ddot{u}(t) + \ddot{u}_g(t)$  are the relative displacement, relative velocity, relative acceleration and the absolute acceleration of the system, respectively. The definitions of response spectra are:  $S_d \equiv |u(t)|_{\max}$  = displacement response spectrum and  $S_a \equiv |\ddot{u}'(t)|_{\max} = |\ddot{u}(t) + \ddot{u}_g(t)|_{\max}$  = (absolute) acceleration response spectrum. Moreover, the pseudo-acceleration response spectrum ( $PS_a$ ) is obtained from the displacement response spectrum ( $S_d$ ) based on the relationship of  $PS_a = \omega^2 S_d$ .

The displacement and acceleration response spectra of Equation (4) can be obtained by using the Duhamel's integral as [14, 15]:

$$S_d \equiv |u(t)|_{\max} = -\frac{1}{\omega\sqrt{1-\zeta^2}} |S(t)|_{\max} \quad (5)$$

$$S_a \equiv |\ddot{u}'(t)|_{\max} = |\omega^2(1-2\zeta^2)u(t) + 2\zeta\omega C(t)|_{\max} \quad (6)$$

where

$$S(t) = \int_0^t \ddot{u}_g(\tau) e^{-\zeta\omega(t-\tau)} \sin \omega_d(t-\tau) d\tau, \quad C(t) = \int_0^t \ddot{u}_g(\tau) e^{-\zeta\omega(t-\tau)} \cos \omega_d(t-\tau) d\tau$$

Comparing  $S_a$  of Equation (6) with  $PS_a = \omega^2 S_d$ , it is clear that  $PS_a$  is exactly equal to  $S_a$  only for the special case of undamped systems. The difference between  $PS_a$  and  $S_a$  becomes apparent if the viscous damping ratio of the system increases.

Figure 2(a) shows the comparison of a mean acceleration response spectrum and a mean pseudo-acceleration response spectrum for various viscous damping ratios. This figure was derived from a total of 1053 earthquake acceleration time histories loaded from the strong motion database of the Pacific Earthquake Engineering Research Center (PEER; <http://peer.berkeley.edu>). All these selected ground motions have the following characteristics: (a) they are recorded in the United States of America; (b) the range of peak ground acceleration (PGA) is from 0.025 to 1.6  $g$ ; (c) the magnitudes of earthquakes are greater than 5.5; and (d) the distances closest to fault rupture range from 0.1 to 180 km. Also, in order to compare the errors between  $PS_a$  and  $S_a$  in detail, the ratios of  $PS_a/S_a$  are given in Figure 2(b). It is clear from Figure 2(b) that  $PS_a$  is nearly the same as  $S_a$  only for those systems where the viscous damping ratio is less than 10% with natural periods shorter than 0.15 sec. The differences increase obviously for systems with higher viscous damping ratios. For example, for the system with a viscous damping ratio of 50% and a natural period of 4.0 sec, the ratio of  $PS_a/S_a$  will

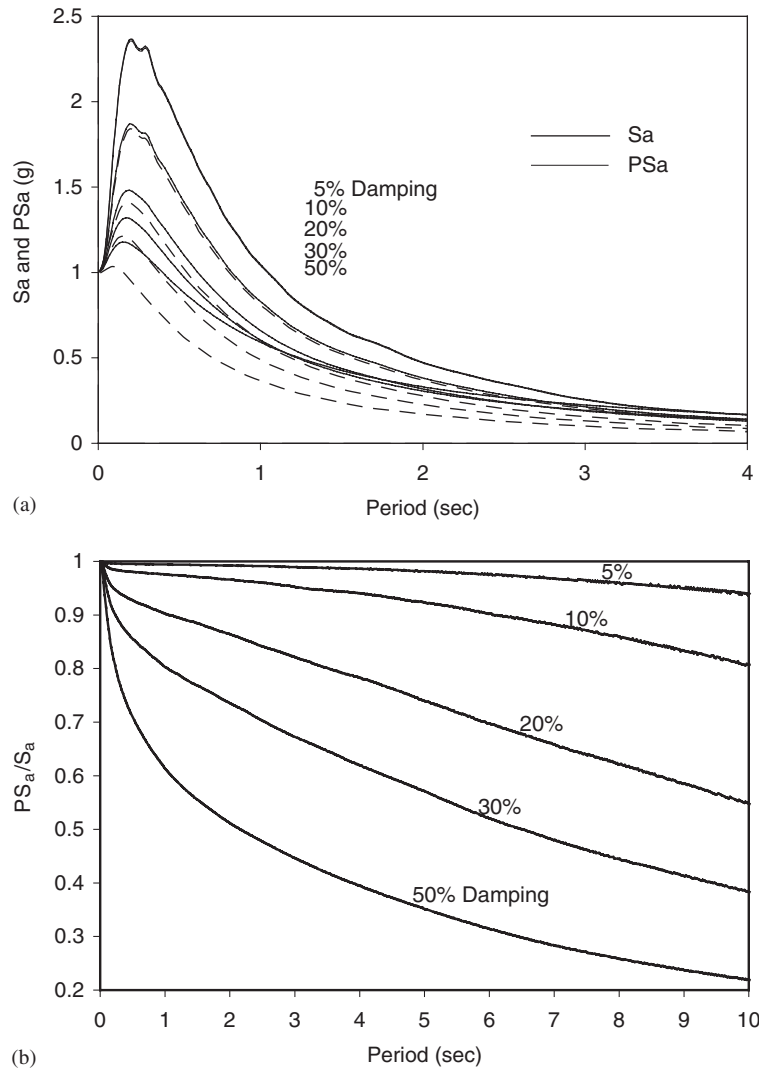


Figure 2. (a) Mean elastic acceleration response spectrum (PGA = 1.0 g).  
 (b)  $PS_a$  normalized by  $S_a$  (i.e.  $PS_a/S_a$ ).

decrease to 0.39, or  $S_a = 2.56 PS_a$ . At this time, if  $PS_a$  is used instead of  $S_a$ , the acceleration responses of the system will be significantly underestimated.

In addition, according to Equation (2), a relationship between ductility ( $\mu$ ) and equivalent viscous damping ratio is plotted in Figure 3. From this figure, it is found that a small ductility ratio always corresponds to a large equivalent viscous damping ratio. For the case of the elastic-perfectly-plastic systems, the viscous damping ratio will be as high as 37% for the system with a ductility ratio of 2. Even for the case of a ductility ratio of 1.5, the viscous

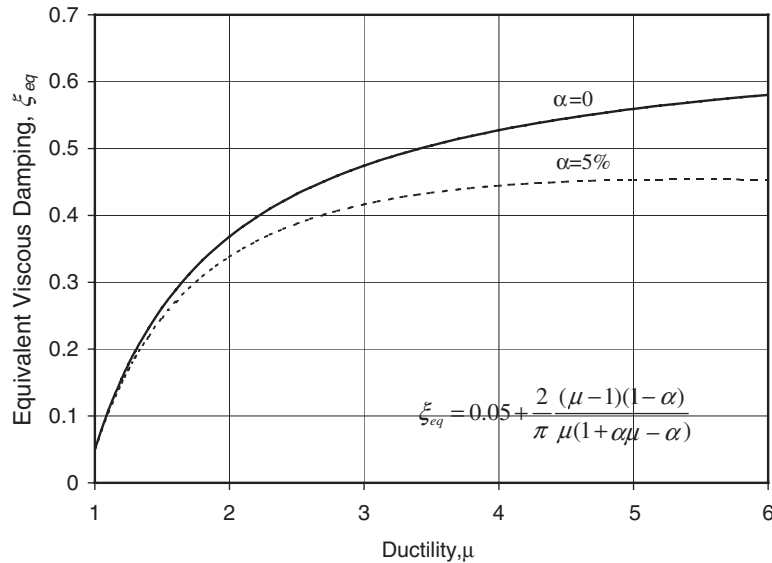


Figure 3. Ductility vs. equivalent viscous damping.

damping ratio also will be 26.2%. These values are obviously too large to affect the iterative results of the capacity spectrum method if the pseudo-acceleration response spectrum ( $PS_a$ ) was used to construct the demand diagram.

#### 4. IMPROVEMENT OF THE CAPACITY SPECTRUM METHOD

Shown in Figure 4 are the demand diagrams plotted by  $S_a$  and  $PS_a$  with damping ratios of 5% and 30%, respectively, for the north–south component of the 1940 El Centro ground motion. Included in the figure are the capacity diagrams of two elastic–perfectly–plastic systems. System I has an elastic natural vibration period  $T_n = 1.0$  sec, a normalized yield strength  $f_y/w = 0.1032$ , and a yield displacement  $u_y = 2.562$  cm. System II has  $T_n = 0.4$  sec,  $f_y/w = 0.22$ , and  $u_y = 0.9$  cm. It can be seen from the figure that the displacement demands ( $D$ ) of System I are 4.43 cm and 11.0 cm corresponding to  $PS_a$  and  $S_a$ , respectively. Similarly, the displacement demands for System II are 3.17 cm ( $PS_a$ ) and 3.74 cm ( $S_a$ ). The two systems get significant errors if  $PS_a$  is used to form the demand diagram. Therefore, in order to improve the accuracy of the capacity spectrum method, it is suggested that the real absolute acceleration response spectrum ( $S_a$ ) be used instead of the pseudo-acceleration response spectrum ( $PS_a$ ) to generate the demand diagram of the capacity spectrum method.

The improved capacity spectrum method for ATC-40 Procedure A is described herein as a sequence of steps:

1. Plot the force–deformation diagram and the 5%-damped elastic response (or design) spectrum, both in the  $A$ – $D$  format (Acceleration–Displacement) to obtain the capacity diagram and 5%-damped elastic demand diagram, respectively. Notice that for the

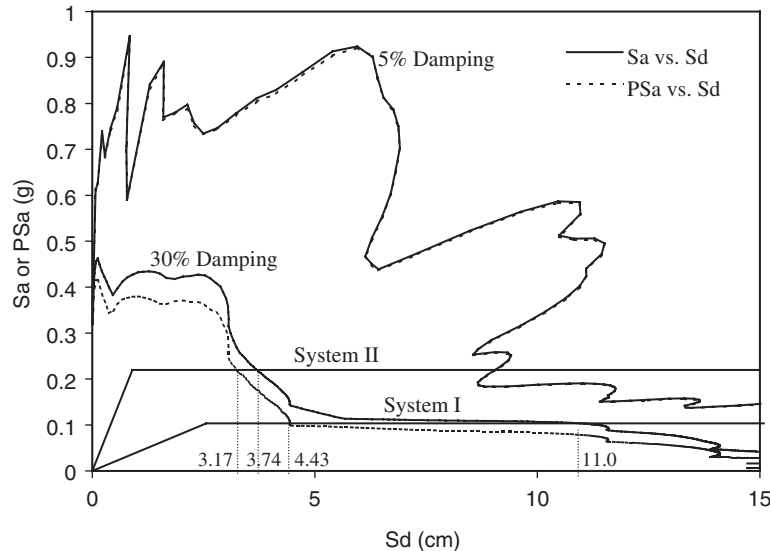


Figure 4. Demand diagram for 1940 El Centro earthquake.

5%-damped systems, the pseudo-acceleration response spectrum ( $PS_a$ ) is almost equal to the acceleration response spectrum ( $S_a$ ). Therefore, in this step, both the ordinate of the pseudo-acceleration response spectrum and that of the acceleration response spectrum can be used as the vertical axis of the 5%-damped elastic demand diagram.

2. Estimate the peak deformation (displacement) demand  $D_i$  and determine the corresponding acceleration  $A_i$  for the capacity diagram. Initially, assume  $D_i = S_d(T_n, \xi = 5\%)$ , determined for period  $T_n$  from the elastic demand diagram.
3. The ductility ratio ( $\mu$ ) can be computed from  $\mu = D_i/u_y$ .
4. By Equation (3), the equivalent damping ratio ( $\xi_{eq}$ ) can be obtained.
5. Plot the elastic demand diagram for  $\xi_{eq}$  determined in Step 4. Notice that in this step, the ordinate of acceleration response spectrum ( $S_a$ ) instead of  $PS_a$  should be used as the vertical axis to form the elastic demand diagram with high damping ratio.
6. Read-off the displacement  $D_j$  where the demand diagram obtained from Step 5 intersects the capacity diagram.
7. Check for convergence. If  $(D_j - D_i) \div D_j \leq \text{tolerance}$ , the earthquake-induced deformation demand  $D = D_j$ . Otherwise, set  $D_i = D_j$  (or another estimated value) and repeat Steps 3–7 until convergence occurs.

## 5. EXAMPLES

The improved procedure is applied to compute the earthquake-induced deformation of six elastic-perfectly-plastic SDOF example systems listed in Table I. The six systems were originally used by Chopra and Goel [7] to discuss the capacity spectrum method of ATC-40. Two values of natural period  $T_n$  are considered. One is 0.5 sec in the acceleration-sensitive spectral

Table I. Properties and response of example systems to the 1940 El Centro earthquake.

	System properties			System response (cm)			
	$T_n$ (s)	$F_y/w$	$u_y$ (cm)	$\mu$	$D_{\text{Chopra,1999}}$	$D_{\text{this paper}}$	$D_{\text{exact}}$
System 1	0.5	0.1257	0.781	6	3.534	4.88	4.65
System 2	0.5	0.1783	1.106	4	3.072	3.65	4.40
System 3	0.5	0.3411	2.117	2	Unconverged	3.31	4.21
System 4	1.0	0.0714	1.773	6	7.192	11.71	10.55
System 5	1.0	0.1032	2.562	4	4.458	8.31	10.16
System 6	1.0	0.1733	4.302	2	Unconverged	5.367	8.53

Table II. The WJE damping model.

$\mu$	1.0	1.25	1.5	2.0	3.0	4.0
$\zeta_{\text{eq}}$ (%) (median + $1\sigma$ )	5.0	7.5	10	14	21	26
$\zeta_{\text{eq}}$ (%) (median)	5.0	8.5	12	16	26	35

region, and the other is 1.0 sec in the velocity-sensitive region. Furthermore, three levels of yield strength and an inherent damping ratio  $\zeta_0$  of 5% for all systems are used in this study. The excitation chosen is the north-south component of the 1940 El Centro ground motion [15]. Detailed steps are presented next for System 1, whereas Table I tabulates the final results of displacement demand (i.e., the earthquake-induced deformation) for all systems.

The improved procedure is illustrated for System 1 as follows:

1. Figure 5 shows the capacity diagram and the 5%-damped elastic demand diagram.
2. Assume an initial displacement demand  $D_i = S_d$  ( $T_n = 0.5$  sec,  $\zeta = 5\%$ ) = 5.69 cm.
3. Ductility  $\mu = D_i/u_y = 5.69/0.781 = 7.30$ .
4. For Type A systems, according to Equation (3),  $\zeta_{\text{eq}} = 0.05 + 0.77 \times 0.45 = 0.40$ .
5. The 40%-damped elastic demand diagram intersects the capacity diagram at  $D_j = 4.88$  cm (Figure 5). As mentioned previously, at this step, the vertical axis of the 40%-damped elastic demand diagram should be the ordinate of the absolute acceleration response spectrum ( $S_a$ ).
6. Difference =  $100 \times (D_j - D_i)/D_j = 100 \times (4.88 - 5.69)/5.69 = -14.2\% > 5\%$  tolerance. Therefore, set  $D_i = 4.88$  and repeat Steps 3 to 6.

For the second iteration,  $D_i = 4.88$  cm,  $\mu = 4.88/0.781 = 6.26$ ,  $\zeta_{\text{eq}} = 0.05 + 0.77 \times 0.45 = 0.40$ . The intersection point is  $D_j = 4.88$  cm and the difference between  $D_i$  and  $D_j$  is 0% which is smaller than the 5% tolerance. Therefore, the iteration process converged at the second cycles. If the pseudo-acceleration response spectrum ( $PS_a$ ) was used to create the 40%-damped elastic demand diagram, the result computed by Chopra and Goel [7] was that the displacement demand of System 1 equals 3.534 cm (Table I). Furthermore, the inelastic time history analysis results give  $D_{\text{exact}} = 4.65$  cm and  $\mu = 6$  for System 1 (Table I). It can be seen from this example

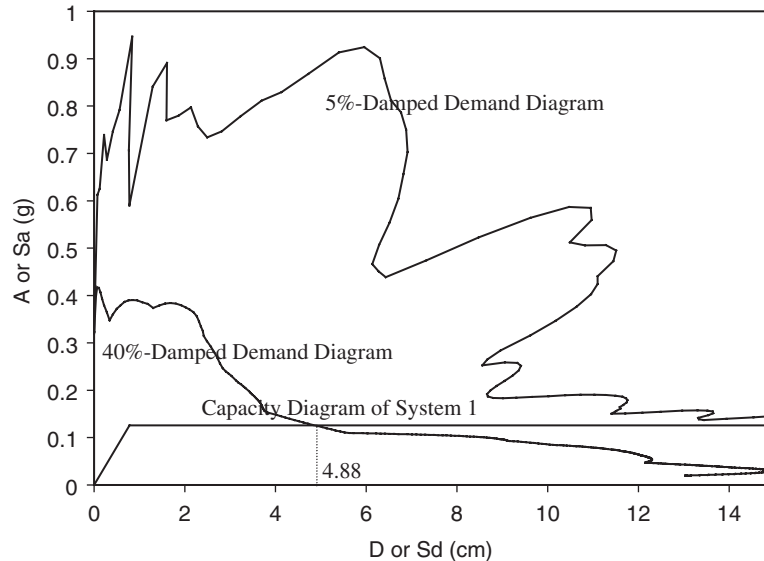


Figure 5. Demand diagram of system 1 for El Centro earthquake.

that the iterative results derived from the acceleration response spectrum ( $S_a$ ) have a much better accuracy than those derived from the pseudo-acceleration response spectrum ( $PS_a$ ).

In addition, as indicated by Chopra and Goel [7], System 3 and System 6 failed to converge in their study (Table I). However, using the improved method, the two systems can obtain converged values (Table I) and all the results of the six systems calculated by the improved procedure are more accurate when compared to the exact results obtained from non-linear time history analysis.

## 6. ACCURACY OF THE CAPACITY SPECTRUM METHOD

For a SDOF elastic-perfectly-plastic system, the accuracy of the iterative results of the capacity spectrum method will depend only on the chosen acceleration response spectrum to form the demand spectrum and the model of the equivalent viscous damping. If  $S_a$  is used to form the demand diagram, then the only factor to affect the accuracy of iterative outcomes is the model of equivalent viscous damping. Although the factor can be thoroughly eliminated by using the inelastic response spectrum [8,9], the equivalent linear systems can still be used to approximately predict the responses of non-linear systems. To respond to the linearization methods, many equivalent viscous damping models have been proposed based on harmonic or earthquake responses [10, 13, 16–18].

In 1979, Iwan and Gates [13] compared the accuracy of nine damping models for defining equivalent linear systems by considering a bilinear hysteretic oscillator. He found that all the existing approximate methods overestimate the equivalent viscous damping for most of the range of ductility considered. However, the average stiffness and energy method (ASE) [13]

gives a relatively uniform low error for the entire range of ductility investigated. Moreover, in 2001, Xue [19] assessed the accuracy of the damping model used in the displacement-based seismic demand evaluation and design of inelastic structures. Five damping models were considered, including the WJE damping model [4, 20] where the error was within 10%. Among others, for structures with a ductility ratio less than 4, the damping model based on the average stiffness and energy method seems to give the most accurate results.

Based on the above descriptions, the ATC-40 damping model for the Type A system, as shown in Equation (2), and the following three damping models will be used to assess the accuracy of six example systems listed in Table I.

1. Average stiffness and energy (ASE) damping model [13]. Based on the earthquake response, the equivalent linear system of this method is defined in terms of average values of stiffness and energy dissipated.

$$\xi_{\text{eq}} = \frac{3}{2\pi\mu^2} \times \frac{2(1-\alpha)(\mu-1)^2 + \pi\xi_0[(1-\alpha)(\mu^2 - \frac{1}{3}) + \frac{2}{3}\alpha\mu^3]}{(1-\alpha)(1 + \ln \mu) + \alpha\mu} \quad (7)$$

where,  $\alpha$  = strain hardening ratio;  $\mu$  = ductility ratio;  $\xi_0$  = inherent damping.

2. The WJE damping model [4, 19, 20], as listed in Table II, is based on the maximum displacement determined from the elastic response spectrum being equal to that obtained from the inelastic response spectrum.
3. The Kowalsky hysteretic damping model [21] was derived based on the Takeda hysteretic model [22], which considers stiffness degradation and energy dissipation in a vibration cycle of the inelastic system and of the equivalent linear system.

$$\xi_{\text{eq}} = \xi_0 + \frac{1}{\pi} \left[ 1 - \mu^n \left( \frac{1-\alpha}{\mu} + \alpha \right) \right] \quad (8)$$

where  $n$  = stiffness degradation factor, with a suggested value of 0 for steel structures and 0.5 for RC structures.

A comparison of  $\xi_{\text{eq}}$  corresponding to the various damping model is plotted in Figure 6 for systems with  $\alpha = n = 0$  and  $\xi_0 = 5\%$ . It is shown that the equivalent viscous damping ratios derived from the ATC-40 damping model are obviously larger than those obtained from the ASE and Kowalsky models. For the six systems (Table I) subjected to the north-south component of the 1940 El Centro earthquake, Table III shows the displacement demand calculated from the ATC-40 Procedure A by using four different damping models. Table IV lists a summary of errors with respect to the solutions of non-linear time-history analyses. It is found that: (a) the ATC-40 damping model underestimates the displacement demand for ductility  $\mu < 5.0$  since it apparently overestimates the equivalent viscous damping caused by non-linear behavior of structures; (b) the WJE damping model gives the most accurate results because it is derived based on the mapping relationship between the elastic and the inelastic response spectrum. Although the WJE damping model has the smallest errors, it is not available for ductility  $\mu > 4.0$  (Table II). Thus, it may be suggested that the WJE damping model be used to calculate the equivalent viscous damping when structures have a ductility ratio  $\mu \leq 4.0$ . On the other hand, the Kowalsky damping model may be implemented when  $\mu > 4.0$ . Alternatively, the Kowalsky damping model may be used to calculate the equivalent viscous damping ratios for the entire range of ductility due to its relatively smaller errors.

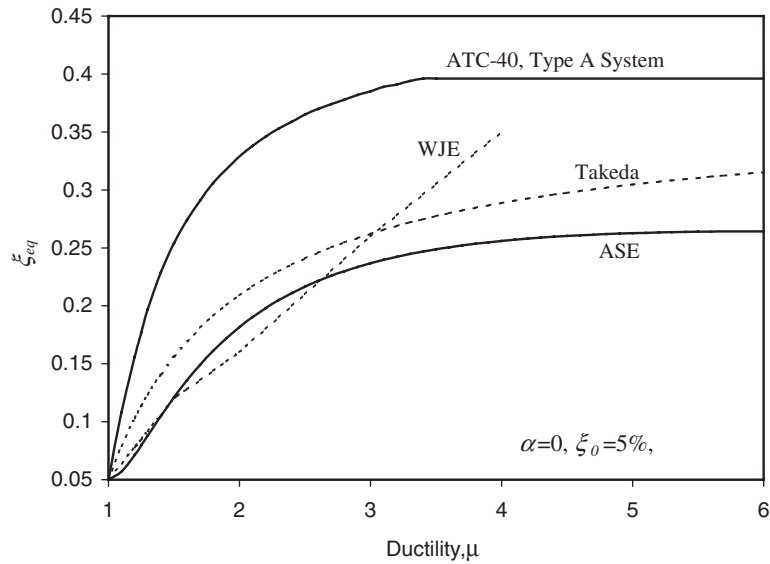


Figure 6. Equivalent viscous damping for various damping models.

Table III. Displacement demands from ATC-40 Procedure A analysis by various damping models (cm).

	ATC-40	ASE	WJE	Kowalsky	Exact
System 1	4.88	5.27		5.07	4.65
System 2	3.65	4.53	4.10	4.32	4.40
System 3	3.31	4.12	4.22	4.00	4.21
System 4	11.71	14.32		12.92	10.55
System 5	8.31	13.06	9.81	11.17	10.16
System 6	5.367	6.62	6.56	6.01	8.53

Table IV. Errors for ATC-40 Procedure A analysis by various damping models.

	ATC-40	ASE	WJE	Kowalsky
System 1	5%	13%		9%
System 2	-17%	3%	-7%	-2%
System 3	-21%	-2%	0%	-5%
System 4	11%	36%		22%
System 5	-18%	29%	-3%	10%
System 6	-37%	-22%	-23%	-30%

## 7. CONCLUSIONS

To trace the iterative procedure of the capacity spectrum method, it is found that the accuracy of its iterative results depends on the chosen acceleration response spectrum to form the demand spectrum and the model of equivalent viscous damping for the SDOF elastic-perfectly-plastic systems. Although these errors can be eliminated by using the inelastic response spectrum, it is still acceptable to use the equivalent linear systems to estimate the responses of non-linear systems. From the results of this study, it has been shown that the iterative results are more accurate when compared to the exact values if  $S_a$  is adopted instead of  $PS_a$  to create the demand diagram. In fact, for a linear system,  $S_a$  is the exact value of the acceleration response but  $PS_a$  is not. Therefore, in order to improve the accuracy of the capacity spectrum method, it is suggested that the real absolute acceleration response spectrum ( $S_a$ ) be used instead of the pseudo-acceleration response spectrum ( $PS_a$ ) to create the demand diagram, especially for systems with  $\zeta_{eq} > 10\%$  and  $T_n > 0.15$  sec.

The equivalent viscous damping model plays another significant role in the capacity spectrum method. If the equivalent damping ratios of the equivalent linear systems are not used appropriately, the displacement demand of structures also will not be accurately estimated even if the real absolute acceleration response spectrum ( $S_a$ ) is used. Since the damping model used by ATC-40 apparently overestimates the equivalent viscous damping ratio caused by the non-linear behavior of structures, this paper recommends that the WJE damping model be used to calculate the equivalent viscous damping ratio when the ductility demand of the structures is less than 4 ( $\mu \leq 4.0$ ), whereas the Kowalsky damping model can be implemented when  $\mu > 4.0$ . Alternatively, the Kowalsky damping model may be used to calculate the equivalent viscous damping for the entire range of ductility due to its relatively smaller overall errors.

## ACKNOWLEDGEMENTS

This study was supported by the National Science Council (NSC-90-2811-Z-002-003) and the Sinotech Engineering Consultant (Grant No. 6120) of Taiwan, R.O.C. The financial support is greatly acknowledged. Moreover, the careful review and comments of two anonymous reviewers is also appreciated.

## REFERENCES

1. ATC-40. *Seismic Evaluation and Retrofit of Concrete Building*. Applied Technology Council, Redwood City, California, 1996.
2. Freeman SA, Nicoletti JP, Tyrell JV. Evaluations of existing buildings for seismic risk—A case study of Puget Sound Naval Shipyard, Bremerton, Washington. *Proceedings of the 1st U.S. National Conference on Earthquake Engineering*, 1975; 113–122.
3. Freeman SA. Prediction of response of concrete buildings to severe earthquake motion. *Publ. SP-55*, American Concrete Institute, Detroit, 589–605, 1978.
4. Freeman SA. Development and use of capacity spectrum method. Paper No. 269. *The 6th U.S. National Conference on Earthquake Engineering/EERI*, Seattle, Washington, 31 May–4 June, 1998.
5. Deierlein GG, Hsieh SH. Seismic response of steel frames with semi-rigid connections using the capacity spectrum method. *Proceedings of the 4th U.S. National Conference on Earthquake Engineering*, vol. 2: 863–872, 1990.
6. Reinhorn AM, Li C, Constantinou MC. *Experimental and analytical investigations of seismic retrofit of structures with supplemental damping*. Report No. NCEER-95-0001, State University of New York at Buffalo, NY, 1995.

7. Chopra AK, Goel RK. *Capacity-demand-diagram methods for estimating seismic deformation of inelastic structures: SDF systems*. Report No. PEER-1999/02, Pacific Earthquake Engineering Research Center, University of California, Berkeley, CA, 1999.
8. Chopra AK, Goel RK. Evaluation of NSP to estimate seismic deformation: SDF systems. *Journal of Structural Engineering* (ASCE) 2000; **126**(4):482–490.
9. Fajfar P. Capacity spectrum method based on inelastic demand spectra. *Earthquake Engineering and Structural Dynamics* 1999; **28**:979–993.
10. Jennings PC. Equivalent viscous damping for yielding structures. *Journal of the Engineering Mechanics Division* (ASCE) 1968; **94**(EM1):103–116.
11. Gulkan P, Sozen M. Inelastic response of reinforced concrete structures to earthquake motions. *ACI Journal* 1974; **71**:604–610.
12. Shibata A, Sozen M. Substitute structure method for seismic design in R/C. *Journal of the Structural Division* (ASCE) 1976; **102**:1–18.
13. Iwan WD, Gates NC. Estimating earthquake response of simple hysteretic structures. *Journal of the Engineering Mechanics Division* (ASCE) 1979; **105**(EM3):391–405.
14. Clough RW, Penzien J. *Dynamics of Structures*. McGraw-Hill: New York, 1993.
15. Chopra AK. *Dynamics of Structures: Theory and Applications to Earthquake Engineering*. Prentice-Hall: New Jersey, 1995.
16. Jacobsen LS. Damping in composite structures. *Proceedings of the 3rd World Conference on Earthquake Engineering* 1960; II:1029–1044.
17. Berg GV. A study of the earthquake response of inelastic systems. *Proceedings of the 34th Convention of the Structural Engineering Association of California*, Coronado, 63–67, 1965.
18. Reddy CK, Pratap R. Equivalent viscous damping for a bilinear hysteretic oscillator. *Journal of Engineering Mechanics* (ASCE) 2000; **126**(11):1189–1196.
19. Xue Q. Assessing the accuracy of the damping model used in displacement-based seismic demand evaluation and design of inelastic structures. *Journal of the Chinese Institute of Engineers*, 2001, submitted.
20. WJE. *Seismic dynamic analysis for building*. Final manuscript prepared for the U.S. Army Engineering Division by Wiss, Janney, Elstner Associates, Inc., Emeryville, California, 1996.
21. Kowalsky MJ, Priestley MJN, MacRae GA. *Displacement-based design, a methodology for seismic design applied to SDOF reinforced concrete structures*. Report No. SSRP-94/16, Structural System Research Project, University of California, San Diego, La Jolla, California, 1994.
22. Takeda T, Sozen MA, Nielson NN. Reinforced concrete response to simulated earthquakes. *Journal of the Structural Division* (ASCE) 1970; **96**:2557–2573.